

CCM Calculations For The Ground-State Properties Of The
One-Dimensional Spin-Half J_1 – J_2 Model:
Possible Evidence of Collinear Ordering for $J_2/J_1 > \frac{1}{2}$?

Damian J.J. Farnell

*Division of Mathematics and Statistics,
Faculty of Advanced Technology, University of Glamorgan,
Pontypridd CF37 1DL, Wales, United Kingdom*

(Dated: January 13, 2013)

Abstract

In this article we investigate the linear-chain spin-half J_1 - J_2 model by using high-order coupled cluster method (CCM) calculations. We employ three model states, namely, a nearest-neighbour (n.n.) Néel model state in which neighbouring spins are antiparallel, a next-nearest-neighbour (n.n.n.) Néel model state in which next-neighbouring spins are antiparallel, and finally a type of “double spiral” model state with *two* pitch angles. For $J_2/J_1 \leq \frac{1}{2}$, we find that the n.n. Néel model state produces the lowest energies. For $J_2/J_1 > \frac{1}{2}$, we find that the stable states for the quantum system are those for the “traditional” spiral state in which the two pitch angles are identical and the collinear n.n.n. Néel model state. As seen previously, we show that we are able to reproduce exactly the dimerised ground (ket) state at the Majumdar-Ghosh point ($J_2/J_1 = \frac{1}{2}$) using the n.n. Néel model state. We show that the onset of the dimerised phase is indicated by a bifurcation of the nearest-neighbour ket- and bra-state correlation coefficients for the nearest-neighbour Néel model state. Furthermore, we show that the n.n.n. Néel model state can also reproduce exactly the dimerized ground (ket) state at the Majumdar-Ghosh point ($J_2/J_1 = \frac{1}{2}$). The ground-state energies for the n.n.n. Néel model state are shown to be much lower than those of the “spiral” model state for a finite region above $J_2/J_1 = \frac{1}{2}$. Indeed, we show that ground-state energies for the collinear n.n. and n.n.n. model states are in good agreement with the results of exact diagonalisations of finite-length chains across this entire regime for $J_1 > 0$. We produce results for the dimer order parameter for $J_2/J_1 > \frac{1}{2}$ by using the n.n.n. Néel model state and these results are in reasonable agreement with previous results of DMRG. Finally, results for the spin-spin correlation functions for the n.n.n. Néel model state are presented. It is shown that the correlation length increases with increasing J_2/J_1 above $J_2/J_1 = \frac{1}{2}$ using this model state and that shift in the peak of the structure function occurs from $q = \pi$ to $q = \pi/2$ as one increases J_2/J_1 . Although these results are not conclusive, they are intriguing because they suggest that a ground state exhibiting collinear order might occur for some region for $J_2/J_1 \geq \frac{1}{2}$.

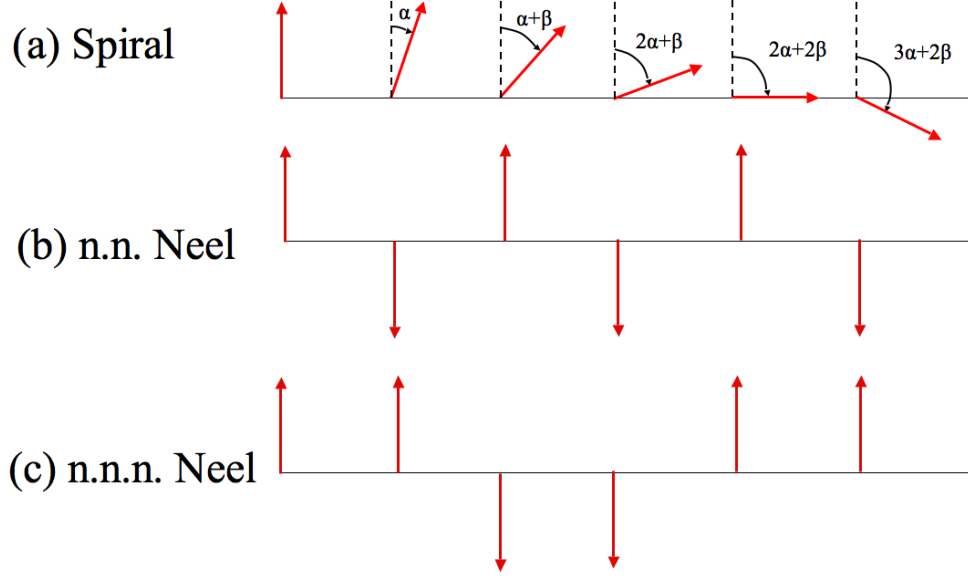


FIG. 1: Model states for the one-dimensional spin-half J_1 - J_2 model. (a) Spiral model states with two angles; (b) collinear nearest-neighbour (n.n.) Néel model state; and, (c) collinear next-nearest-neighbour (n.n.n.) Néel model state

I. INTRODUCTION

The formation of dimer- and plaquette-ordered singlet ground states (so-called valence-bond crystal (VBC) states) is an interesting and important topic in quantum spin systems. Often, the formation of enhanced dimer or plaquette correlations is driven by frustration, which can increase quantum fluctuations and which may result in such gapped rotationally-invariant quantum paramagnetic states. An example for the appearance of such exact VBC product eigenstates are the spin-half J_1 - J_2 model on the linear chain [1-12] at the point $J_2/J_1 = \frac{1}{2}$ (the so-called Majumdar-Ghosh point), which is an example of spontaneous symmetry breaking.

The Hamiltonian for this spin-half model has nearest-neighbour (n.n.) bonds of strength J_1 and next-nearest-neighbour (n.n.n.) bonds of strength J_2 is given by

$$H = \frac{J_1}{2} \sum_{i, \rho_1} \mathbf{s}_i \cdot \mathbf{s}_{i+\rho_1} + \frac{J_2}{2} \sum_{i, \rho_2} \mathbf{s}_i \cdot \mathbf{s}_{i+\rho_2} \quad , \quad (1)$$

where the index i runs over sites on the lattice, ρ_1 runs over all nearest-neighbours to i , and ρ_2 runs over all next-nearest-neighbours to i . Henceforth we put $|J_1| = 1$ and consider $J_2 \geq 0$.

The ground-state properties of this system have been studied using methods such as exact diagonalizations [2,7], DMRG [3-5,9], CCM [8-11], and field-theoretical approaches [5] (see Refs. [5,6] for a general review). At $J_2/J_1 = 0$ we have the unfrustrated Heisenberg antiferromagnet, where the exact solution is provided by the Bethe Ansatz. The ground state is gapless and the spin-spin correlation function $\langle \mathbf{s}_i \cdot \mathbf{s}_j \rangle$ decays slowly to zero according to a power-law, i.e. no true Néel-like long-range order is observed. In the region $J_2/J_1 > 0$ the nearest-neighbour (J_1) and next-nearest-neighbour interactions (J_2) compete, thus leading to frustration. At $J_2/J_1 = 0.2411(1)$ the model exhibits a transition to a two-fold degenerate gapped dimerized phase with an exponential decay of the correlation function $\langle \mathbf{s}_i \cdot \mathbf{s}_j \rangle$ [2-6]. This state breaks the translational lattice symmetry. At the Majumdar-Ghosh point $J_2/J_1 = \frac{1}{2}$ there are two degenerate simple exact dimer-singlet product ground states corresponding to the dimerized product state for the Hamiltonian of Eq. (1) [1]. The ground state for $J_2/J_1 > \frac{1}{2}$ is not completely well-understood, although it is known that gap [5] persists for some range above $J_2/J_1 = \frac{1}{2}$ and that incommensurate spiral correlation occur. Furthermore, DMRG studies suggest that a Lifschitz point occurs at $J_2/J_1 = 0.52$ and that the dimer order parameter peaks at $J_2/J_1 = 0.58$. In the limit $J_2/J_1 \rightarrow \infty$, the system decouples into two Bethe chains and so the system is gapless.

II. METHOD

A. The CCM Formalism

A description of the underlying methodology for the CCM is given in Refs. [13-21]. We note here that the ket and bra ground-state energy eigenvectors, $|\Psi\rangle$ and $\langle\tilde{\Psi}|$, of a general many-body system described by a Hamiltonian H

$$H|\Psi\rangle = E_g|\Psi\rangle ; \quad \langle\tilde{\Psi}|H = E_g\langle\tilde{\Psi}| , \quad (2)$$

are parametrised within the single-reference CCM as follows:

$$\begin{aligned} |\Psi\rangle &= e^S |\Phi\rangle ; \quad S = \sum_{I \neq 0} \mathcal{S}_I C_I^+ , \\ \langle\tilde{\Psi}| &= \langle\Phi| \tilde{S} e^{-S} ; \quad \tilde{S} = 1 + \sum_{I \neq 0} \tilde{\mathcal{S}}_I C_I^- . \end{aligned} \quad (3)$$

Note that $|\Phi\rangle$ is the normalised single model or reference state. The correlation operator S is thus a linked-cluster operator that is decomposed in Eq. (3) in terms of a complete set

of mutually commuting multi-spin and multi-configurational creations operators C_I^+ with respect to the model state. The hermitian adjoints, $C_I^- = (C_I^+)^\dagger$ are the corresponding destruction operators, $\langle \Phi | C_I^+ = 0 = C_I^- | \Phi \rangle$, and we explicitly define $C_0^+ = 1$, the identity operator. The label I is thus a set-index comprising a set of single-particle labels in some suitable single-particle basis defined via $|\Phi\rangle$. We note that the normalisation conditions $\langle \Phi | \Psi \rangle = \langle \Phi | \Phi \rangle = 1 = \langle \tilde{\Psi} | \Psi \rangle$ follow from Eq. (3). The ground ket- and bra-state equations are given in terms of $\bar{H} = \langle \tilde{\Psi} | H | \Psi \rangle$ as

$$\delta \bar{H} / \delta \tilde{\mathcal{S}}_I = 0 \Rightarrow \langle \Phi | C_I^- e^{-S} H e^S | \Phi \rangle = 0, \forall I \neq 0 ; \quad (4)$$

$$\delta \bar{H} / \delta \mathcal{S}_I = 0 \Rightarrow \langle \Phi | \tilde{S} e^{-S} [H, C_I^+] e^S | \Phi \rangle = 0, \forall I \neq 0 . \quad (5)$$

In order to solve for the one-dimensional J_1 - J_2 model considered here, we make approximations in both S and \tilde{S} . The three most commonly employed approximation schemes previously utilised have been: (1) the SUB n scheme, in which all correlations involving only n or fewer spins are retained, but no further restriction is made concerning their spatial separation on the lattice; (2) the SUB n - m sub-approximation, in which all SUB n correlations spanning a range of no more than m adjacent lattice sites are retained; and (3) the localised LSUB m scheme, in which all multi-spin correlations over all distinct locales on the lattice defined by m or fewer contiguous sites are retained. Equation (4) shows that the ground-state energy at the stationary point has the simple form

$$E_g = E_g(\{\mathcal{S}_I\}) = \langle \Phi | e^{-S} H e^S | \Phi \rangle . \quad (6)$$

In this article we focus on the application of high-order (CCM) [22-24] to the spin-half, one-dimensional J_1 - J_2 model. The CCM calculations were carried out to high-order using a computational code written by us [25]. The first CCM analyses [8,9] concentrated the Néel model state with neighbouring spins antiparallel [8] and then for a spiral model state [8,9] in which there is a pitch angle between neighbouring spins. It was assumed that translational symmetry was preserved in both cases, and these calculations led to good results for the ground-state energies of this system. In Refs. [10,11], we used a “doubled” unit cell including two neighbouring sites for this spin-half system on the linear chain at points (0,0,0) and (1,0,0) and a single Bravais vector $(2,0,0)^T$ to take into account the symmetry breaking. There are thus two distinct types of two-spin nearest-neighbor ket-state correlation coefficients, namely, those connecting the sites inside the unit cell and

those connecting different unit cells. These coefficients are denoted as \mathcal{S}_2^a and \mathcal{S}_2^b , and it is straightforward [10, 11] to prove that the ground state at $J_2/J_1 = \frac{1}{2}$ is obtained *exactly* by setting $\mathcal{S}_2^a = 1$ and all other coefficients equal to zero. Interestingly, a similar exact ground state at $J_2/J_1 = \frac{1}{2}$ may also be formed for the n.n.n. Néel model state and again $\mathcal{S}_2^a = 1$ and all other correlation coefficients are zero.

We use three model states, namely, a spiral model state, and n.n. and n.n.n. Néel model states, shown in Fig. 1. For all of these model states, we rotate the spin coordinates of the ‘up’ spins so that notationally they become ‘down’ spins in these locally defined axes. For example, the relevant Hamiltonian in these rotated coordinates for the model state (a) is then given by

$$H = \sum_{\langle i \rightarrow j \rangle} J_{i,j} \left\{ \cos(\theta_{i,j}) s_i^z s_j^z + \frac{1}{4} (\cos(\theta_{i,j}) + 1) (s_i^- s_j^+ + s_i^+ s_j^-) + \frac{1}{4} (\cos(\theta_{i,j}) - 1) (s_i^+ s_j^+ + s_i^- s_j^-) + \frac{1}{2} \sin(\theta_{i,j}) ((s_i^- s_i^+) s_j^z - s_i^z (s_j^- + s_j^+)) \right\} \quad (7)$$

where $\theta_{i,j}$ is the difference between pitch angles at sites i and j . Furthermore, we see for model state (a) that $\theta_{2i,2i+1} = \alpha$, $\theta_{2i+1,2i+2} = \beta$, and $\theta_{i,i+2} = \alpha + \beta$ where $i = 0, 1, 2, \dots$. (We note also that $J_{i,i+1} = J_1$ and $J_{i,i+2} = J_2$.) We remark that both model states (b) may be obtained from model state (a) by setting $\alpha = \beta = \pi$ and model state (c) by $\alpha = \pi$ and $\beta = 0$. Model state (a) allows us to investigate the stability of the collinear n.n. and n.n.n. model states, as well as the special case $\alpha = \beta$ previously considered in Refs. [8,9].

III. RESULTS

For $J_2/J_1 \leq \frac{1}{2}$, the n.n. Néel state is found to yield the best results. For $J_2/J_1 \geq \frac{1}{2}$, there were found to be two stable solutions with respect to the “pitch” angles α and β , namely: the collinear n.n.n. Néel model state ($\alpha = \pi$ and $\beta = 0$ or vice versa), which breaks the symmetry of the lattice; and, a spiral state with $\alpha = \beta$, which therefore does not break the translational symmetry of the lattice. We may plot the angle $\alpha(=\beta)$ for the spiral solution, and this is shown in Fig. 2. We see that the spiral solution is “lost” at around $J_2/J_1 \approx 0.7$, as noted previously in Ref. [9]. There is a direct and finite step-change to $\alpha = \pi$ at this point. Furthermore, we see slight oscillations in α for $J_2/J_1 \lesssim 1$. It is unclear why this should occur, although perhaps this behaviour may indicate some rapid change in the ground state and/or that the model state is becoming increasingly inappropriate.

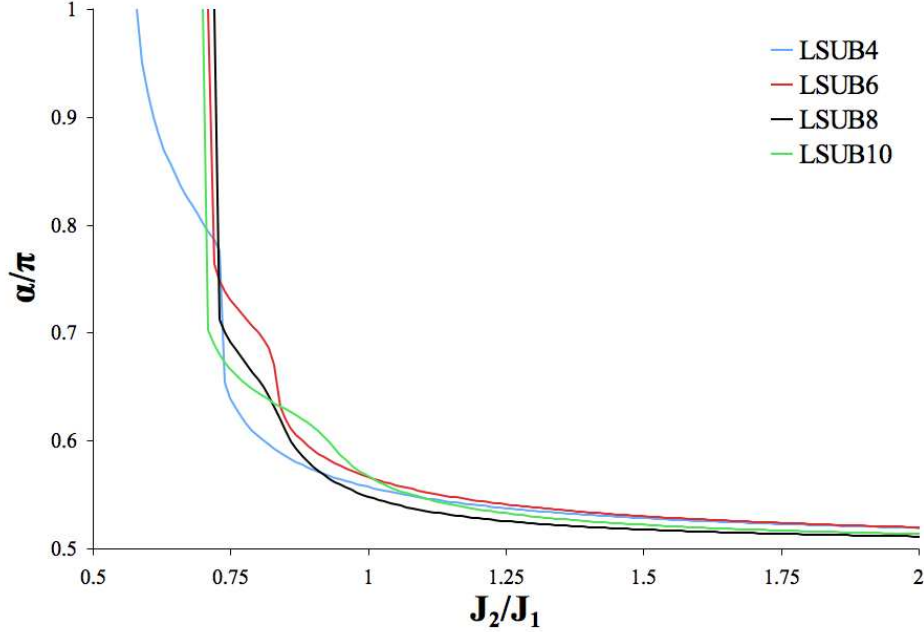


FIG. 2: Results for the pitch angle $\alpha(=\beta)$ versus J_2/J_1 for the spiral model state (a).

We may investigate these solutions further by fixing the value of β and then varying α , see Fig. 3. For the n.n.n. Néel model state, we may set $\beta = 0$ for all values of J_2/J_1 and we see from this figure that the minimum energy solution is given by $\alpha = \pi$ in this case (i.e., identically model state (c)). Furthermore, we may set the value of β to be given by the value shown in Fig. 2 (at a given level of LSUB m approximation and for a given value of J_2/J_1) in order to investigate the “spiral” case. We note that the stable minimal solution is given by $\alpha = \beta$, which preserves the translational symmetry of the lattice. Note that no other intermediate solutions, e.g., a kind of double spiral in which $\beta = 0$ and $\alpha \neq \pi$ were seen to occur. For $J_2/J_1 > \frac{1}{2}$, there was either the translational symmetry-breaking case of model state (c) or the spiral state with $\alpha = \beta$, which preserves translational symmetry.

We remark that the n.n. Néel model state (b) (i.e., $\alpha = \beta = \pi$) generally better produces for $J_2/J_1 \leq \frac{1}{2}$ than the n.n.n. Néel model state (c), and vice versa in the region $J_2/J_1 \geq \frac{1}{2}$. Results for the ground-state energies as a function of J_2/J_1 are shown in Fig. 4. Of the collinear model states (b) and (c), results for the n.n. Néel model state (b) are shown for $J_2/J_1 < \frac{1}{2}$ and those of the n.n.n. Néel model and (c) for $J_2/J_1 > \frac{1}{2}$. Exactly at the MG point $J_2/J_1 = \frac{1}{2}$, we find that these two states have equal energy. Furthermore, this solution is the CCM symmetry-broken solution (more is said of this below), which forms an exact ket

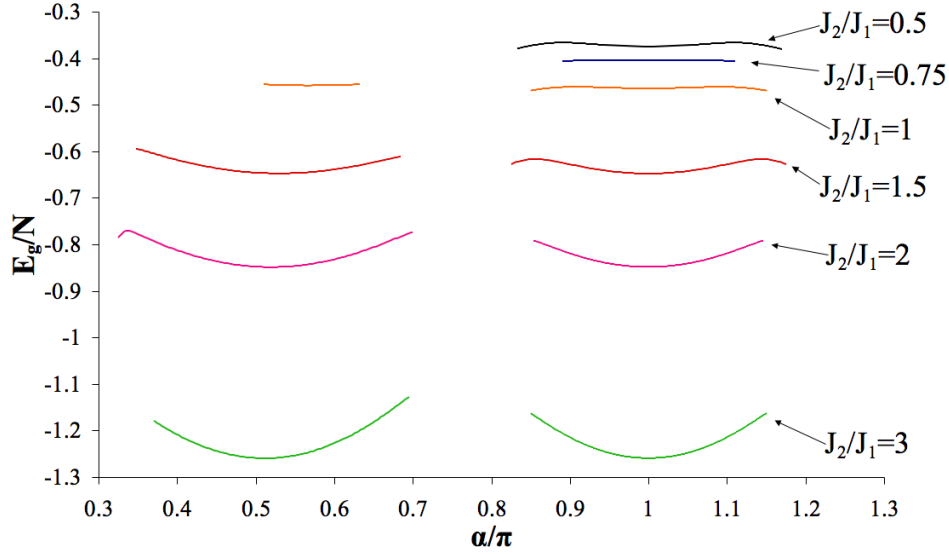


FIG. 3: Results for the CCM ground-state energy versus pitch angle α as a function of J_2/J_1 at the LSUB6 level of approximation. Results on the right of the figure are for $\beta = 0$ (so are for the n.n.n. Néel model state (c)) and those on the left are for β given in Fig. 2 are so are for the spiral case.

eigenstate at this point. For $J_2/J_1 \geq \frac{1}{2}$, we find that the $\alpha = \pi$ and $\beta = 0$ (i.e., model state (c)) is lowest until $J_2/J_1|_{c_2}$ equal to 1.02, 1.69, 1.29, and 1.76 at the LSUB4 to LSUB10 levels of approximation respectively. (The non-monotonic behaviour of this crossing is probably due to a “double” odd/even effect, where the “doubled” comes from the range of the J_2 bonds.) Above this point, the energies for the spiral model state (a) with $\alpha = \beta$ appear to be lower. Symmetry breaking might therefore persist for some region for $J_2/J_1 \geq \frac{1}{2}$. The differences between the energies of these two states above this crossover point are very small however, e.g., it is of order 10^{-4} at the LSUB10 approximation. The difference only becomes large for $J_2/J_1 < J_2/J_1|_{c_2}$, where the symmetry-breaking n.n.n. Néel collinear model state (c) is clearly much lower than the spiral solution for $\alpha = \beta$. Furthermore, it is possible that the crossover goes to higher and higher values of J_2 with increasing level of LSUBm approximation level. However, we cannot rule out the possibility that another state of more “exotic” order that is not accessible from the model states used here might occur just above $J_2/J_1 = \frac{1}{2}$. If so then this state might exhibit lower ground-state energies.

Henceforth, we concentrate on results for the collinear n.n. Néel model state (b) for

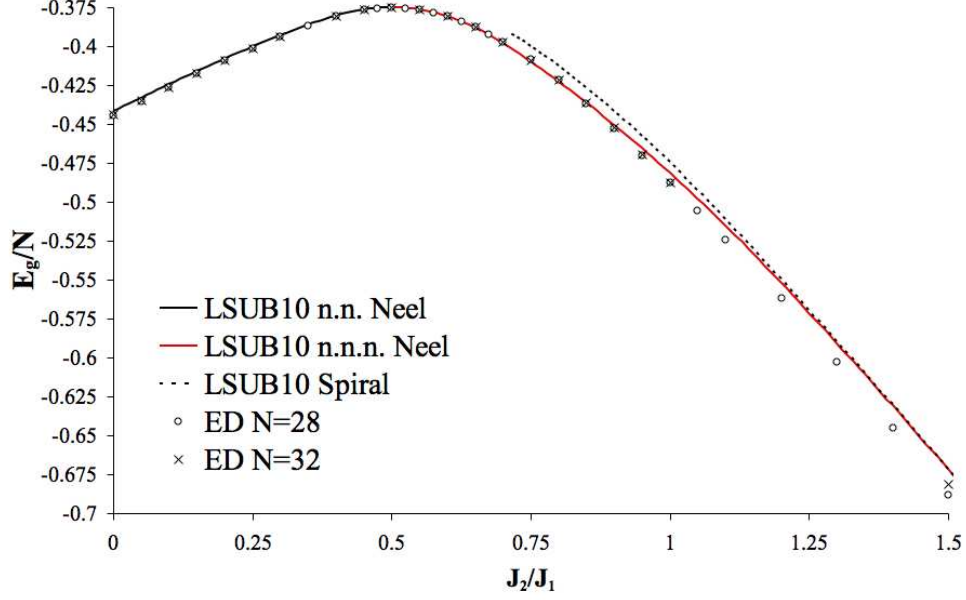


FIG. 4: Results for the CCM ground-state energy as a function of J_2/J_1 for the collinear n.n. Néel model state (b) (for $J_2/J_1 \leq \frac{1}{2}$) and n.n.n. Néel model state (c) (for $J_2/J_1 \geq \frac{1}{2}$) and the spiral model state (a) with $\alpha = \beta$.

$J_2/J_1 \leq \frac{1}{2}$ and the collinear n.n.n. Néel model and (c) only for $J_2/J_1 \geq \frac{1}{2}$. Results for the ket-state correlation coefficients for the n.n. and n.n.n. Néel model states (b) and (c) are shown as a function of J_2/J_1 in Fig. 5. We remark again that both model states (b) and (c) provide an exact solution at $J_2/J_1 = \frac{1}{2}$, namely, where $\mathcal{S}_2^a = 0$ and all other ket-state correlation coefficients are zero. Starting from $J_2/J_1 = \frac{1}{2}$ we were able to track this exact solution (as seen previously also in Refs. [10,11]) within a certain LSUB m approximation for the n.n. Néel model state to lower values of $J_2/J_1 \leq \frac{1}{2}$. It was also found previously [10,11] that the solution (i.e. $\mathcal{S}_2^a = \mathcal{S}_2^b$) having the full translational symmetry [8,9] was the only solution below a critical point $J_2/J_1|_{c_1} (< \frac{1}{2})$. Above this point the CCM solution for the n.n. correlation coefficient bifurcates, as shown in Fig. 5. CCM results for the ground-state for the symmetry-breaking solution to the CCM equations for $J_2/J_1 > J_2/J_1|_{c_1}$ compared better to exact diagonalisation results in this regime than those results for the “usual n.n. (‘Néel-type’) solution” that do not break translation symmetries (see Refs. [10,11] for more details.) However, as was also noted before [10,11], the value for $J_2/J_1|_{c_1}$ is much too large (e.g., $J_2/J_1|_{c_1} = 0.436$ at the for LSUB14 level of approximation). This value ought to be compared to the value of $J_2/J_1 = 0.2411(1)$ the model exhibits a transition to a two-fold

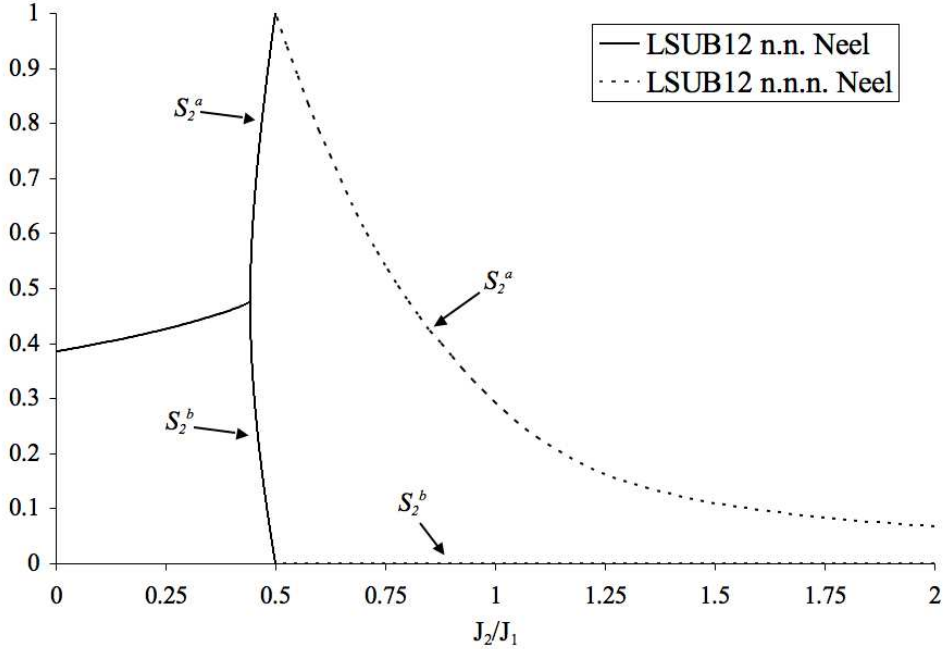


FIG. 5: Results for the CCM ket-state correlation coefficients at the LSUB12 level of approximation for the one-dimensional spin-half J_1 – J_2 model using the collinear nearest-neighbour (n.n.) Néel model state and the collinear next-nearest-neighbour (n.n.n.) Néel model state.

degenerate gapped dimerized phase.

As we increase the level of approximation the value for $J_2/J_1|_{c_1}$ does seem to decrease, albeit slowly. In Ref. [11], it was proposed that results for the predicted energy gap at a given level of LSUB m approximation are overestimated, with good results given only after extrapolation. This might artificially stabilise the “usual CCM solution” that preserves translational symmetry and that is known to be gapless. Hence $J_2/J_1|_{c_1}$ might be grossly overestimated. However, it is fair to say that this proposition is mostly speculation. We believe however that the detection of any such “symmetry-breaking” solutions via the CCM is strong point of the method.

We note again that the exact solution at $J_2/J_1 = \frac{1}{2}$ may be obtained for the n.n.n. Néel model state (c) by setting $\mathcal{S}_2^a = 1$ and all other coefficients equal to zero. This solution may be tracked for $J_2/J_1 > \frac{1}{2}$ and the results for the n.n. ket-state correlation coefficients are also shown in Fig. 5. We remark again that this is the minimum energy solution compared to the “spiral” solution up to some possible cross-over value $J_2/J_1|_{c_2}$. Importantly, the ket-state correlation coefficient \mathcal{S}_2^a is non-zero (and \mathcal{S}_2^b is zero) for all values of $J_2 > \frac{1}{2}$ for this model

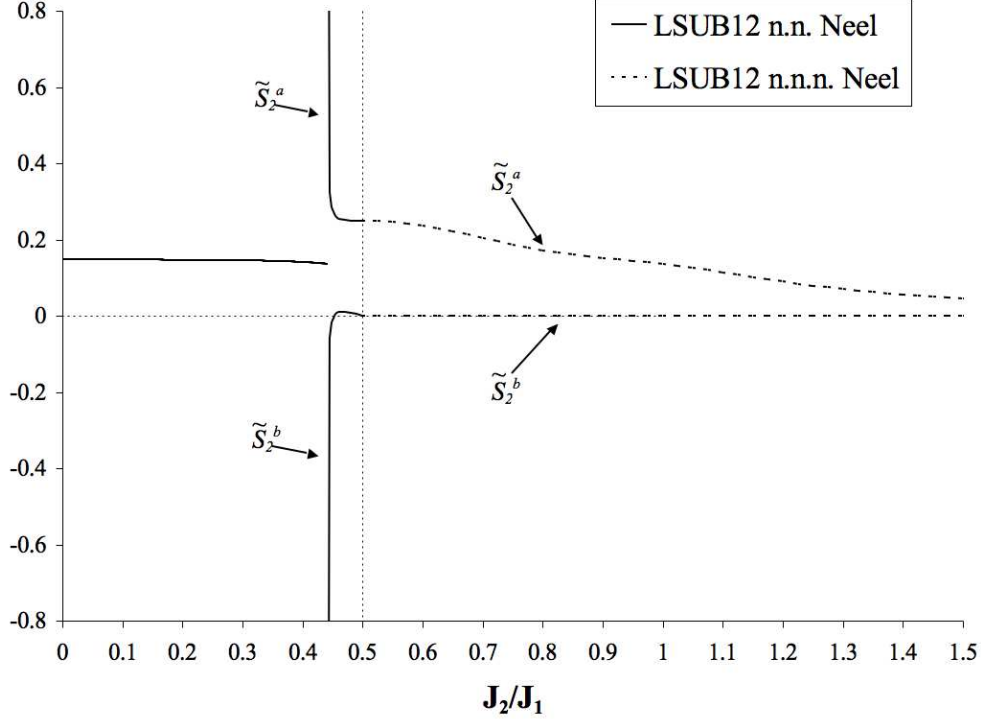


FIG. 6: Results for the CCM bra-state correlation coefficients at the LSUB12 level of approximation for the one-dimensional spin-half J_1 - J_2 model using the collinear nearest-neighbour (n.n.) Néel model state and the collinear next-nearest-neighbour (n.n.n.) Néel model state.

state, which suggests that the symmetry-broken ground state might persist for some range of $J_2/J_1 (\gtrsim \frac{1}{2})$.

The nearest-neighbor bra-state correlation coefficient at the LSUB m level of approximation at $J_2/J_1 = \frac{1}{2}$ has $\tilde{S}_2^a = 1/4$ with $m \geq 4$. This is shown in Fig. 6 for the LSUB12 level of approximation. We find that the nearest-neighbor correlation coefficient diverges as $J_2/J_1 \rightarrow J_2/J_{1c_1}$ and this is also shown in Fig. 6. Again, the usual (‘Néel-type’) solution ($\tilde{S}_2^a = \tilde{S}_2^b$) is obtained for $J_2/J_1 < J_2/J_{1c_1}$. Again, a similar solution at $J_2/J_1 = \frac{1}{2}$ may also be found for n.n.n. Néel model state (c), again for which $\tilde{S}_2^a = 0.25$ and all other coefficients equal to zero. In the limit $J_2/J_1 \rightarrow \infty$, the bra-state correlation coefficient \tilde{S}_2^a goes to zero. Once more, qualitatively similar results are observed at other levels of LSUB m approximation for the bra-state correlation coefficients as a function of J_2/J_1 .

The dimer order parameter is given by $d = \langle \mathbf{s}_{2i} \cdot (\mathbf{s}_{2i+1} - \mathbf{s}_{2i-1}) \rangle$. We find this quantity for the n.n.n. Néel model state and the results for $J_2 > \frac{1}{2}$ are shown in Fig. 7. Results for the n.n. Néel model state show an unphysical divergence at the critical point

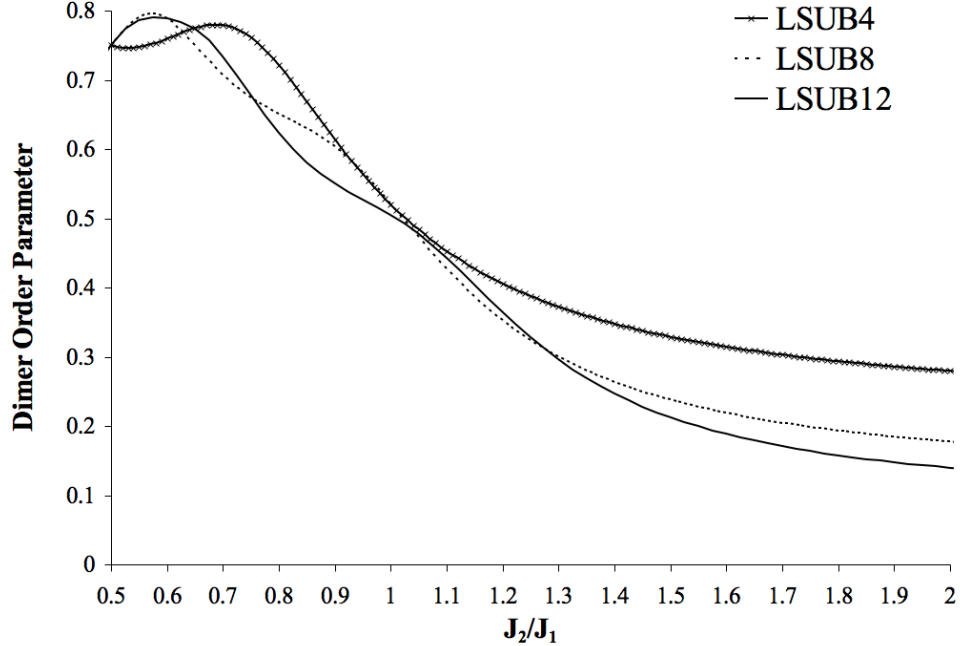


FIG. 7: Results for the dimer order parameter for the one-dimensional spin-half J_1 - J_2 model using the collinear next-nearest-neighbour (n.n.n.) Néel model state.

$J_2/J_1|_{c_1}$, which is due to a divergence in the NCCM bra-state correlation coefficients as shown above. (This is uninteresting and so is not shown here.) We remark that there is a maximum in d near to $J_2/J_1 \approx 0.6$. For example, at the LSUB12 level of approximation, there is a maximum value of the dimer order parameter d of $d = 0.790$ at $J_2/J_1 = 0.58$. This compares well to the results of DMRG in Refs. [5,9] by visual comparison. In particular, it was noted in Ref. [9] that the maximum in d occurs at $J_2/J_1 = 0.58$, in agreement with these new CCM results. The results for the n.n.n. Néel model state appear to decay to zero in the limit $J_2/J_1 \rightarrow \infty$, as expected. However, they do not seem to agree (at given LSUB m level of approximation) with the results of DMRG [5] that predict a decay of d given by $d = 2.283\exp(-1.622J_2/J_1)$. Furthermore (and somewhat troublingly), the CCM results also show unphysical oscillations in d as one varies J_2/J_1 . The reason for this is unclear, although it might hint at strong changes occurring in the in the ground state at this point and/or that the n.n.n. Néel model state is possibly a poor choice. However, it is probably still fair to say that the CCM results for the dimer order parameter broadly follow the same pattern as in Ref. [5,9], although quantitative agreement for large J_2/J_1 is very poor. Higher orders of approximation and/or extrapolation might solve this problem.

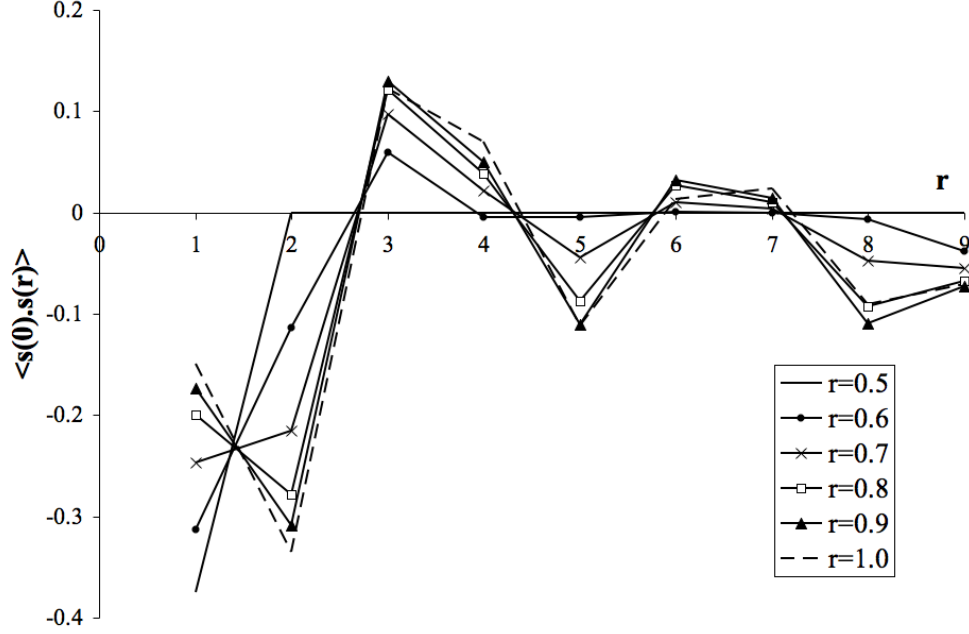


FIG. 8: Results for the spin-spin correlation function via the CCM for the one-dimensional spin-half J_1-J_2 model using the collinear next-nearest-neighbour (n.n.n.) Néel model state at the LSUB12 level of approximation.

Spin-spin correlation functions may be found for the n.n.n. Néel model state (c). At LSUB12 these results are found to be converged to roughly a separation of $r \approx 10$, shown in Fig. 8, and at LSUB14 they are found to be converged to roughly a separation of $r \approx 12$. Note however that convergence is also somewhat affected by the value of J_2/J_1 , with convergence with increasing level of LSUB m levels of approximation being quicker at lower values of J_2/J_1 . The correlation length ϵ may be found [5] by fitting the form $ax^{-0.5} \exp(-x/\epsilon) \cos(\theta x + \lambda)$ to the spin-spin correlation functions for the n.n.n. Néel model state (c) and these results plotted as a function of J_2/J_1 in Fig. 9 at the LSUB10 to LSUB14 levels of approximation. By visual inspection only, these results at the LSUB14 level of approximation do not appear to compare too badly to those of DMRG presented in Ref. [5]. Indeed, the correlation length does seem to increase with increasing J_2/J_1 . This is an interesting result for a collinear model state of the type given by the n.n.n. Néel model state (c), although some caution should be exercised in interpreting these results because we again include results for results only up to $r = 8$ at LSUB10, $r = 10$ at LSUB12, and $r = 12$ at LSUB12. We see that the discrepancy between the predicted correlation lengths

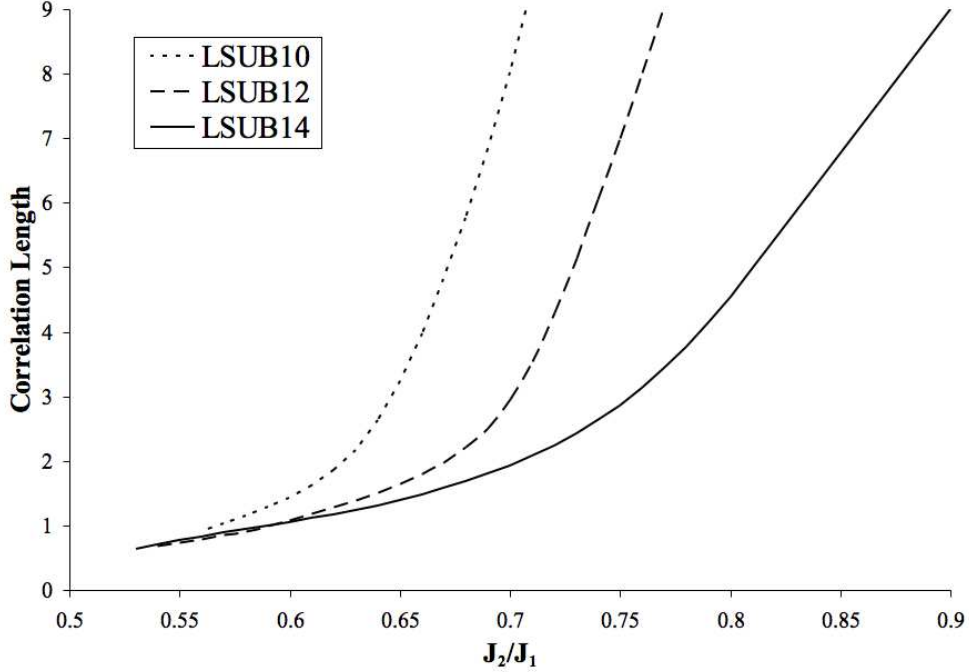


FIG. 9: Results for the correlation length via the CCM for the one-dimensional spin-half J_1 - J_2 model using the collinear next-nearest-neighbour (n.n.n.) Néel model state at the LSUB10 to LSUB14 levels of approximation.

between LSUB10, LSUB12, and LSUB14 becomes larger as J_2/J_1 increases. However, all levels of approximation indicate an increase in the correlation length with increasing J_2/J_1 , as expected.

The static structure function may be defined by

$$C(q) = \frac{1}{2} \sum_{r=-\infty}^{r=+\infty} \langle s(\mathbf{0}) \cdot s(\mathbf{r}) \rangle e^{i\mathbf{r} \cdot \mathbf{q}} \quad (8)$$

However, again our localised LSUB m approximation will function correctly only for a restricted range of r . Results for the static structure function at LSUB14 are shown in Fig. 9. We see that the peak of the structure function moves from $q = \pi$ at $J_2/J_1 = 0.5$ to $q = \pi/2$ for larger values of J_2/J_1 . This is in reasonable agreement with previous results of Ref. [9] that shows a similar shift in the peak, which was interpreted as indicating spiral order. However, the present results indicate that such a change can occur for a model state with collinear n.n.n. ordering also. By visual comparison, the heights of the peaks shown in Fig. 10 are in reasonable qualitative agreement with those shown in Fig. 4 of Ref. [9]. We remark that characteristic and strong oscillations are seen at the LSUB14 level of approximation

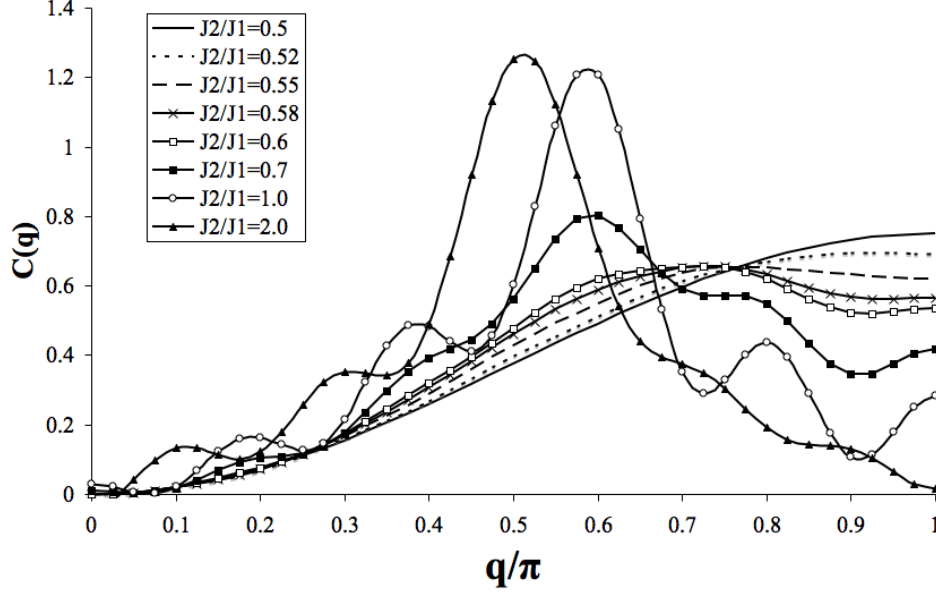


FIG. 10: Results for the static structure function $C(q)$ via the CCM for the one-dimensional spin-half J_1 – J_2 model using the collinear next-nearest-neighbour (n.n.n.) Néel model state at the LSUB14 level of approximation.

for $J_2/J_1 \approx 1$. This might be the model state is a poor choice in this regime, although it is more likely that it is because we need to truncate the range r for the LSUB m scheme. Indeed, similar oscillations are seen in Fig. 4 of Ref. [9] and these are most probably due to finite-size effects.

IV. CONCLUSIONS

In this article, CCM results were presented for the spin-half 1D J_1 – J_2 model. We saw that the n.n. Néel model state provided good results for $J_2/J_1 \leq \frac{1}{2}$. In particular, a translational symmetry-breaking solution was shown to provide good results for the symmetry-broken phase for this model that exhibits a gap (see also Refs. [10,11]). However, as remarked previously elsewhere [10,11] the value for the onset of this phase $J_2/J_1|_{c_1} = 0.2411$ was shown to be overestimated by this approach. The stability of the (non-collinear) spiral and (collinear) n.n.n. Néel model states were examined by using a model state that could interpolate between the two model states (and incidentally also the n.n. Néel model state). It was found for $J_2/J_1 \geq \frac{1}{2}$ that the only stable solutions were for the case of the “non-

translational-symmetry-breaking” spiral and the (symmetry-breaking) n.n.n. Néel model state. All other intermediate cases seemed not to be stable. Interestingly, the ground-state energies for these two states were extremely close for large range of J_2/J_1 . However, the spiral case appeared to be slightly lower in the limit of large values of J_2/J_1 . Even more startlingly, however, the energies for the collinear n.n.n. Néel model state became lower than for the spiral case in the regime $\frac{1}{2} \lesssim J_2/J_1 \lesssim 2$. This hints at a possible “order-from-disorder” phenomena in this model in this regime. However, these results should be treated with caution because the “true” ground state in this regime might still be quite different to any of the states studied here.

Results for the dimer order parameter d using the n.n.n. Néel model state showed a maximum at d at about $J_2/J_1 \approx 0.58$ (of $d \approx 0.79$ at the LSUB12 level of approximation), which was in good agreement with DMRG results of Ref. [9]. The decay of d with increasing J_2/J_1 did not agree with DMRG results and also the CCM results also demonstrated “oscillations” in d as one varied J_2/J_1 . The n.n.n. nature of the J_2 bond means that the length scale is effectively doubled and so we probably need to go to much higher levels of LSUB m approximation via massive parallel processing. In order to achieve good quantitative agreement for large J_2/J_1 , we might also need to extrapolate our LSUB m results in the limit $m \rightarrow \infty$. However, it is probably still fair to say that the CCM results for the dimer order parameter d showed here followed a broadly similar pattern to results of DMRG of Refs. [5,9],

The presence of collinear n.n.n. Néel ordering some region for $J_2/J_1 > \frac{1}{2}$ seems to contradict earlier results of other approximate method that indicate incommensurate spiral correlations commonly (see, e.g., Ref. [9]), i.e., possibly suggesting some form of “spiral” ground state. Spiral ordering is suggested because the classical spiral ground state must also show a similar change position of the peak in the (classical) structure function. However, we note that our results the static structure function for the n.n.n. Néel model (e.g., at the LSUB14 level of approximation in Fig. 10) state also showed a distinct peak that moved from $q = \pi$ at $J_2/J_1 = \frac{1}{2}$ to $q = \pi/2$ as $J_2/J_1 \rightarrow \infty$. This was also seen in DMRG studies [9] of the quantum system. Furthermore, CCM results here predict that the correlation length becomes larger as one increases J_2/J_1 in the regime $J_2/J_1 > \frac{1}{2}$, again as was also seen in DMRG studies [5]. Note however that we used a fairly restricted range in r for the spin-spin correlation functions in order to form our results for the structure function etc. (only up to a separation of $r \approx 10, 12$ at LSUB14 for the structure function). This fact does

not bolster our confidence in our results, although this approach ought to be adequate in the regime just above $J_2/J_1 = \frac{1}{2}$, where the correlation length is known to be very short-ranged.

In conclusion, the results presented in this article present an intriguing (though ultimately inconclusive) possibility that collinear n.n.n. Néel ordering might occur for $J_2/J_1 > \frac{1}{2}$. The ground-state energies for the n.n.n. Néel model state are lowest and results for the dimer order parameter, correlation length and structure function using this model state are (arguably) predicted correctly. If this result is in fact true then it has a number of implications for the interpretation of similar evidence (e.g., from structure functions) in other systems where the existence incommensurate “spiral” ordering is inferred. We suggest that other approximate methods (e.g., spin-wave theory and cumulant series expansions) might be applied to the 1D J_1 – J_2 model using a n.n.n. Néel state as a “starting point”. We recommend also that even higher-order CCM be carried out using massive parallel processing in order to confirm the results presented here.

-
- [1] C.K Majumdar and D.K. Ghosh, J. Math. Phys. **10**, 1388 (1969); J. Math. Phys. **10**, 1399 (1969).
 - [2] T. Tonegawa and I. Harada, J. Phys. Soc. Japan **56**, 2153 (1987).
 - [3] K. Nomura and K. Okamoto, Phys. Lett. **169A**, 433 (1992); J. Phys. Soc. Japan **62**, 1123 (1993); J.Phys. A.: Math. Gen. **27**, 5773 (1994).
 - [4] R. Chitra, S. Pati, H.R. Krishnamurthy, D. Sen, and S. Ramasesha, Phys. Rev. B **52**, 6581 (1995).
 - [5] S. R. White and I. Affleck, Phys. Rev. B **54**, 9862 (1996).
 - [6] H.-J. Mikeska and A. K. Kolezhuk, in *Quantum Magnetism*, Lecture Notes in Physics **645**, U. Schollwöck, J. Richter, D.J.J. Farnell, and R.F. Bishop, eds. (Springer-Verlag, Berlin, 2004), pp 1-83.
 - [7] A.A. Aligia, C.D. Batista, and F.H.L. Eßler, Phys. Rev. B **62**, 3259 (2000).
 - [8] D.J.J. Farnell and J.B. Parkinson, J. Phys.: Condens. Matter **6**, 5521 (1994).
 - [9] R. Bursill, G.A. Gehring, D.J.J. Farnell, J.B. Parkinson, T. Xiang, and C. Zeng, J. Phys.: Condens. Matter **7**, 8605 (1995).
 - [10] D.J.J. Farnell, J. Richter, R. Zinke, and R.F. Bishop, J. Stat. Phys. **135**, 175-198 (2009).

- [11] D.J.J. Farnell, *Condensed Matter Theories* – in print.
- [12] R. Zinke, S.-L. Drechsler, and J. Richter, *Phys. Rev. B* **79**, 094425 (2009)
- [13] F. Coester, *Nucl. Phys.* **7**, 421 (1958); F. Coester and H. Kümmel, *ibid.* **17**, 477 (1960).
- [14] J. Čížek, *J. Chem. Phys.* **45**, 4256 (1966); *Adv. Chem. Phys.* **14**, 35 (1969).
- [15] R.F. Bishop and K.H. Lührmann, *Phys. Rev. B* **17**, 3757 (1978); *ibid.* **26**, 5523 (1982).
- [16] H. Kümmel, K.H. Lührmann, and J.G. Zabolitzky, *Phys Rep.* **36C**, 1 (1978).
- [17] J.S. Arponen, *Ann. Phys. (N.Y.)* **151**, 311 (1983).
- [18] R.F. Bishop and H. Kümmel, *Phys. Today* **40(3)**, 52 (1987).
- [19] J.S. Arponen, R.F. Bishop, and E. Pajanne, *Phys. Rev. A* **36**, 2519 (1987); *ibid.* **36**, 2539 (1987); in: *Condensed Matter Theories*, Vol. **2**, P. Vashishta, R.K. Kalia, and R.F. Bishop, eds. (Plenum, New York, 1987), p. 357.
- [20] R.J. Bartlett, *J. Phys. Chem.* **93**, 1697 (1989).
- [21] R.F. Bishop, *Theor. Chim. Acta* **80**, 95 (1991).
- [22] C. Zeng, D.J.J. Farnell, and R.F. Bishop, *J. Stat. Phys.* **90**, 327 (1998).
- [23] R.F. Bishop, D.J.J. Farnell, S.E. Krüger, J.B. Parkinson, J. Richter, and C. Zeng, *J. Phys.: Condens. Matter* **12**, 6887 (2000).
- [24] D.J.J. Farnell, R.F. Bishop, and K.A. Gernoth, *J. Stat. Phys.* **108**, 401 (2002).
- [25] For the numerical calculation we use the program package ‘Crystallographic Coupled Cluster Method’ of D.J.J. Farnell and J. Schulenburg, see <http://www-e.uni-magdeburg.de/jschulen/ccm/index.html>.